This is a repository copy of *Performance-based Seismic Design of Flexible-Base Multi-Storey Buildings Considering Soil-Structure Interaction*.

White Rose Research Online URL for this paper:
http://eprints.whiterose.ac.uk/92601/

Version: Accepted Version

Article:
Lu, Y., Hajirasouliha, I. and Marshall, A.M. (2016) Performance-based Seismic Design of Flexible-Base Multi-Storey Buildings Considering Soil-Structure Interaction. Engineering Structures, 108. 90 - 103. ISSN 1873-7323

https://doi.org/10.1016/j.engstruct.2015.11.031

Article available under the terms of the CC-BY-NC-ND licence
(https://creativecommons.org/licenses/by-nc-nd/4.0/)

Reuse
Unless indicated otherwise, fulltext items are protected by copyright with all rights reserved. The copyright exception in section 29 of the Copyright, Designs and Patents Act 1988 allows the making of a single copy solely for the purpose of non-commercial research or private study within the limits of fair dealing. The publisher or other rights-holder may allow further reproduction and re-use of this version - refer to the White Rose Research Online record for this item. Where records identify the publisher as the copyright holder, users can verify any specific terms of use on the publisher's website.

Takedown
If you consider content in White Rose Research Online to be in breach of UK law, please notify us by emailing eprints@whiterose.ac.uk including the URL of the record and the reason for the withdrawal request.

eprints@whiterose.ac.uk
https://eprints.whiterose.ac.uk/

Lu Y, Hajirasouliha I & Marshall A (2016). Performance-based Seismic Design of Flexible-Base Multi-Storey Buildings Considering Soil-Structure Interaction. Engineering Structures, Vol 108, 90-103.

Performance-based Seismic Design of Flexible-Base Multi-Storey Buildings Considering Soil-Structure Interaction

Yang Lu[1*], Iman Hajirasouliha[2], Alec M. Marshall[1]

[1] *Department of Civil Engineering, The University of Nottingham, UK*

[2]*Department of Civil & Structural Engineering, The University of Sheffield, UK*

[*]*Corresponding Author: E-mail: evxyl7@nottingham.ac.uk*

Abstract

A comprehensive parametric study has been carried out to investigate the seismic performance of multi-storey shear buildings considering soil-structure interaction (SSI). More than 40,000 SDOF and MDOF models are designed based on different lateral seismic load patterns and target ductility demands to represent a wide range of building structures constructed on shallow foundations. The cone model is adopted to simulate the dynamic behaviour of an elastic homogeneous soil half-space. 1, 5, 10, 15 and 20-storey SSI systems are subjected to three sets of synthetic spectrum-compatible earthquakes corresponding to different soil classes, and the effects of soil stiffness, design lateral load pattern, fundamental period, number of storeys, structure slenderness ratio and site condition are investigated. The results indicate that, in general, SSI can reduce (up to 60%) the strength and ductility demands of multi-storey buildings, especially those with small slenderness ratio and low ductility demands. It is shown that code-specified design lateral load patterns are more suitable for long period flexible-base structures; whereas a trapezoidal design lateral-load pattern can provide the best solution for short period flexible-base structures. Based on the results of this study, a new design factor R_F is introduced which is able to capture the reduction of strength of single-degree-of-freedom structures due to the combination of SSI and structural yielding. To take into account multi-degree-of-freedom effects in SSI systems, a new site and interaction-dependent modification factor R_M is also proposed. The R_F and R_M factors are integrated into a novel performance-based design method for site and interaction-dependent seismic design of flexible-base structures. The adequacy of the proposed method is demonstrated through several practical design examples.

Key Words: Soil-Structure Interaction; Strength Reduction Factor; Ductility; Multi-Storey Shear-Building; Nonlinear Analysis; Performance-Based Design; Site Class

1 Introduction

While flexible foundations can affect the seismic responses of structures, current seismic codes either allow engineers to take advantage of Soil-Structure Interaction (SSI) by using a reduced response spectrum [1], or permit SSI effects to be neglected for common building structures [2]. This concept stems from the fact that the SSI effect increases the period of the system, which usually leads to a reduced design acceleration spectrum, and also provides additional energy dissipation capacity due to the soil material damping and radiation [3].

Several studies have been performed to investigate the effects of SSI on the seismic response of Single-Degree-of-Freedom (SDOF) structures using elasto-plastic oscillators supported by soil springs. Some studies [4, 5] have reported beneficial SSI effects, while others [6, 7] have shown opposite results. It has been generally accepted that the predominant period of the site motion plays an important role in SSI analyses [8, 9]. Beneficial SSI effects have been found for structures with natural periods higher than the site period, whereas detrimental effects are observed in structures whose periods are shorter than the site period. This implies that neglecting SSI effects in the seismic design procedures does not necessarily lead to conservative design solutions.

While a number of investigations have been conducted to study the strength-ductility relationship of SDOF SSI systems [10-12], less attention has been paid to the inelastic strength demands of Multi-Degree-of-Freedom (MDOF) SSI systems. Santa-Ana and Miranda [13] studied the base shear strength relationship between MDOF and their corresponding SDOF systems using site-dependent ground motions. However, the compliance of the foundation was not included in their analysis. In a more recent study, Ganjavi and Hao [14] investigated the strength-ductility relationship of flexible-base multi-storey shear buildings subjected to a group of 30 real earthquake ground motions recorded on alluvium and soft soil deposits. Based on their results, a new equation was proposed to estimate the strength reduction factor for MDOF SSI systems. Based on a study on seismic response of SSI systems utilising a nonlinear Winkler-based model, Raychowdhury [15] concluded that foundation nonlinearity can reduce

the ductility demands of buildings. Aydemir and Ekiz [16] studied the ductility reduction factor for flexible-base multi-storey frames subjected to 64 earthquake ground motions that were categorised into 4 groups according to the U.S. geological survey site classification system. They observed that the ductility reduction factor values for flexible-base frame systems are generally smaller than the code-specified values, especially for softer soil conditions.

As is well known, seismic design of building structures in modern codes and provisions is based on elastic response spectra derived for lightly damped fixed-base SDOF oscillators. Therefore, the code design response spectra cannot be directly used for seismic design of flexible-base structures with SSI effects. To address this issue, there is a need to provide a link between inelastic seismic demands of flexible-base multi-storey buildings and code design spectra for fixed-base SDOF systems. For the first time, this study aims to provide such a link through a comprehensive parametric analysis using an analytical model to study the seismic response of flexible-base inelastic multi-storey buildings under design spectrum-compatible earthquakes. To this end, a large number of nonlinear 1, 5, 10, 15 and 20-storey SSI models, representing a wide range of buildings founded on shallow foundations, are utilised to assess the seismic performance of flexible-base structures subjected to design spectrum-compatible earthquakes corresponding to different soil conditions. The effects of soil stiffness, design lateral load pattern, fundamental period, number of storeys, structure slenderness ratio and site condition on the structural strength and ductility demands are investigated. The results of the SSI systems subjected to code spectrum-compatible earthquakes in the parametric study are then used to develop a novel performance-based design approach for seismic design of flexible-base multi-storey buildings considering the effects of SSI and site conditions. By introducing new strength and MDOF reduction factors for SSI systems, the suggested design methodology only requires information from fixed-base SDOF elastic design spectra that are available from seismic design guidelines. The proposed design methodology is, therefore well suited for practical applications.

The paper is organised into seven main sections. An outline of the adopted analysis methods is presented first, followed by an assessment the effect of influential parameters. The limitations of existing strength reduction and MDOF modification factors are then illustrated. The following sections present the newly proposed strength reduction and MDOF modification factors, which are then used in

a novel approach for performance-based seismic design of MDOF SSI systems. Finally, the efficiency of the proposed method is demonstrated through several design examples.

2 Modelling and Assumptions

2.1 Soil-Structure Interaction Model

Shear-building models, despite some limitations, have been widely adopted in seismic analyses of multi-storey buildings (e.g. [17, 18]) due to their capability of capturing both nonlinear behaviour and higher mode effects without compromising the computational effort, which makes them suitable for large parametric studies. In shear-building models, each floor is idealised as a lumped mass m connected by elastic-perfectly-plastic springs that only experience shear deformations when subjected to lateral forces, as shown in Fig. 1(a). The height-wise distribution of stiffness and strength in shear building models are assumed to follow the same pattern as storey shear forces derived from the design lateral load pattern [17, 18]. This implies that the yield displacement (= storey strength/ storey stiffness) is considered to be constant at all storey levels. It should be noted that the design parameters to define shear-building models can be obtained based on the results of a single push-over analysis on the fixed-base structure [18]. To accomplish this, a pushover analysis is conducted on the fixed-base frame structure and the relationship between the storey shear force and the total inter-storey drift is extracted. The nonlinear force-displacement relationships are then replaced with an idealised bi-linear relationship to calculate the nominal stiffness, strength, and yield displacement of each storey. The storey ductility can then be calculated as the ratio of maximum inter-storey drift to the storey yield displacement. The ductility demand of the multi-storey building is defined as the maximum of the inter-storey ductility ratios. In this study, the total mass of each building was uniformly distributed along its height, and the height h between floors was assumed to be 3.3m. Rayleigh damping was applied to the shear-building models with a damping ratio of 5% assigned to the first mode and to the mode at which the cumulative mass participation exceeded 95%.

A discrete-element model was used to simulate the dynamic behaviour of a rigid circular foundation overlying a homogenous soil half-space. This model is based on the idealization of homogeneous soil

under a base mat by a semi-infinite truncated cone [19], and its accuracy has been found to be adequate for practical applications compared to more rigorous solutions [20]. The stiffness of the supporting soil was modelled through a sway and rocking cone model (see Fig. 1(b)), whose properties are given by Wolf [21] as follows:

$$k_h = \frac{8\rho V_s^2 r}{2-\nu}, c_h = \rho V_s \pi r^2 \tag{1}$$

$$k_\theta = \frac{8\rho V_s^2 r^3}{3(1-\nu)}, c_\theta = \frac{\rho V_p \pi r^4}{4} \tag{2}$$

$$M_\theta = 0.3\left(\nu - \frac{1}{3}\right)\pi\rho r^5, M_\varphi = \frac{9}{128}(1-\nu)\pi^2\rho r^5\left(\frac{V_p}{V_s}\right)^2 \tag{3}$$

where k_h, k_θ and c_h, c_θ are the equivalent stiffness (denoted by k) and radiation damping coefficient (denoted by c) for the horizontal (denoted with subscript h) and rocking (denoted with subscript θ) motions, respectively. The homogeneous soil half-pace beneath the circular surface foundation with a radius r is defined by its mass density ρ, Poisson's ratio ν, shear wave velocity V_s and dilatational wave velocity V_p. For simplicity, each floor of the superstructure was assumed to have an equivalent radius r, so that the centroidal moment of inertia of each floor and the foundation are, respectively, J=0.25mr^2 and J_f=0.25$m_f r^2$, where m_f is the mass of the foundation, which was set to ten percent of the total mass of the superstructure.

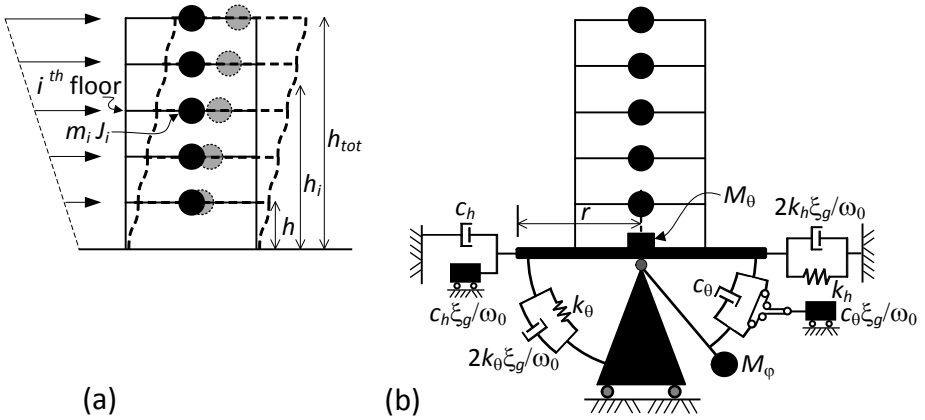

Fig. 1. (a) Typical shear building model; and (b) Simplified SSI model

An additional rotational degree of freedom φ, with its own mass moment of inertia M_φ, is introduced so that the convolution integral embedded in the foundation moment-rotation relation can be

satisfied in the time domain [21]. It should be noted that for nearly incompressible soil (i.e. $1/3< \nu \leq 1/2$), the use of V_p would overestimate the rocking radiation damping. This is remedied by adding a mass moment of inertia M_θ to the rocking degree of freedom and replacing V_p by $2V_s$ [21]. The material damping of the soil half-space is also modelled by augmenting each of the springs and dashpots with an additional dashpot and mass, respectively [22]. In this study, the soil material damping ratio ξ_g=5% was specified at the lowest Eigen-frequency ω_0 of an SSI system, which can be calculated iteratively according to Veletsos and Nair [23] and Luco and Lanzi [24]. Frequency-dependent impedance functions proposed by Veletsos and Verbic [25] were used to derive ω_0, which was solved iteratively by increasing the frequency of vibration from zero (i.e. static condition) to $10V_s/r$ until both frequencies were equal within 0.1 percent (i.e. $|\omega-\omega_{ssi}|\leq 0.001$). It is worth mentioning that some seismic guidelines (e.g. [26, 27]) enable the strain-compatible shear wave velocities of soil to be determined from their small-strain counterparts by using a site and earthquake intensity dependent stiffness degradation relationship. In this way, soil nonlinearity can be approximated using the equivalent linear method if the strain-compatible damping is also available.

2.2 Design Load Patterns, Fundamental periods and Earthquakes

The lateral seismic force distributions in most building codes (e.g. [28, 29]) follow a pattern which is similar to the first-mode deflected shape of lumped MDOF elastic systems. In general, the design lateral force F_i at storey i can be expressed as:

$$F_i = \frac{w_i h_i^k}{\sum_{j=1}^{N} w_j h_j^k} V \tag{4}$$

where V is the total design base shear; w_i and h_i are the effective weight and height of the floor at level i from the ground, respectively; N is the number of storeys; and the exponent k is a function of the building's fundamental period (T_n) which is mainly used to take into account higher mode effects [30]. In the present study, six different lateral load patterns were considered for seismic design of multi-storey shear buildings. A comparison of the distributions of these lateral seismic forces is shown in Fig. 2(a) with their k values presented in Table 1. Fig. 2(b) illustrates the height-wise storey shear force distributions of a 10-storey building with T_n = 1 sec for the adopted load patterns.

Table 1. Lateral load patterns used in this study

Lateral load pattern	Exponent k
Concentric	N/A (A single load applied at roof)
Rectangular	0
Trapezoidal	$0.5+0.2T_n$
Eurocode 8	1
IBC-2012	$\begin{cases} 1, & if\ T_n < 0.5 \\ 2, & if\ T_n > 2.5 \\ 1+0.5(T_n-0.5), & other\ T_n \end{cases}$
Parabolic	$1+0.8T_n$

According to ASCE 7-10 [31], the fundamental period of an MDOF structure can be approximated by using the following formula:

$$T_n = C_t h_{tot}^x \tag{5}$$

where h_{tot} is the total height of the structure, while the coefficients C_t and x are related to the type of the structural system, as presented in Table 2.

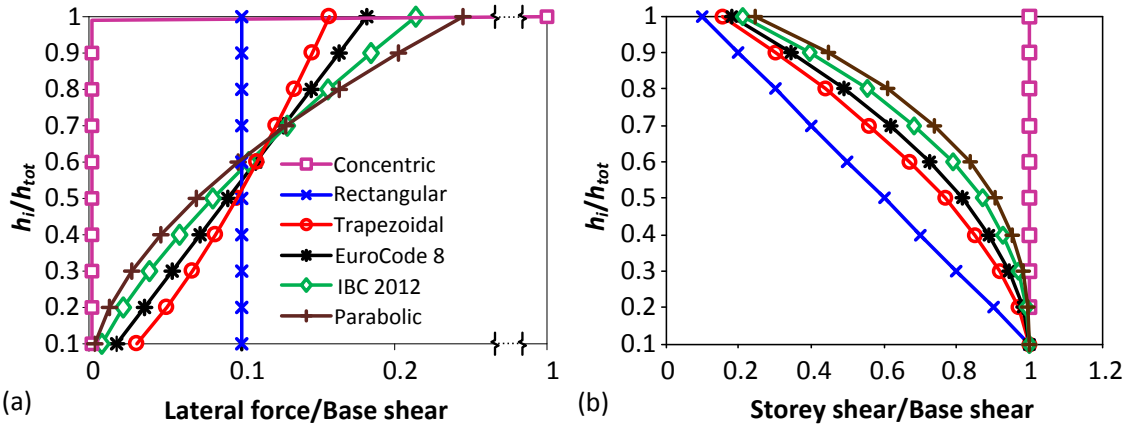

Fig. 2. Comparison of (a) lateral force distributions; and (b) storey shear force distributions for the adopted design load patterns. Examples are shown for the case with N=10 and T_n=1 sec.

Table 2. C_t and x parameters for different structural systems according to ASCE 7-10 [31]

Structural Type	C_t	x
1 Steel moment-resisting frames	0.0724	0.8
2 Concrete moment-resisting frames	0.0466	0.9
3 Steel eccentrically braced/Steel buckling-restrained braced frames	0.0731	0.75
4 All other structural systems	0.0488	0.75

In the current design codes, the soil sites are generally classified into several broad categories according to an average shear wave velocity measured from the top surface of a site to a depth of tens of meters. For example, in IBC-2012 [28] the average shear wave velocity of the top 30 meters of a soil deposit, $V_{s,30}$, is used to identify different soil classes, as shown in Table 3. In this study, to investigate the effect of site condition on the strength-ductility relationship of SSI systems, three sets of spectrum-compatible synthetic earthquakes were used to represent the IBC-2012 design response spectra corresponding to soil classes C, D and E (see Table 3). Each set of the synthetic earthquakes consists of fifteen seismic excitations with a Peak Ground Acceleration (PGA) of 0.4g. These ground motions were generated artificially by using the SIMQKE program [32] based on pseudo-random phasing with a time-varying modulating function. Similar records were also used by Hajirasouliha and Pilakoutas [30] to identify the optimum design load distribution for seismic design of regular and irregular shear-buildings. It is shown in Fig. 3 that the average acceleration response spectrum of synthetic earthquakes in each set compares very well with its corresponding IBC-2012 design spectrum. The characteristic periods of the design ground motions T_0 are also shown in Fig. 3 with the values given in Table 3. This period represents the transition point from acceleration-controlled to the velocity-controlled segment of a 5% damped design spectrum.

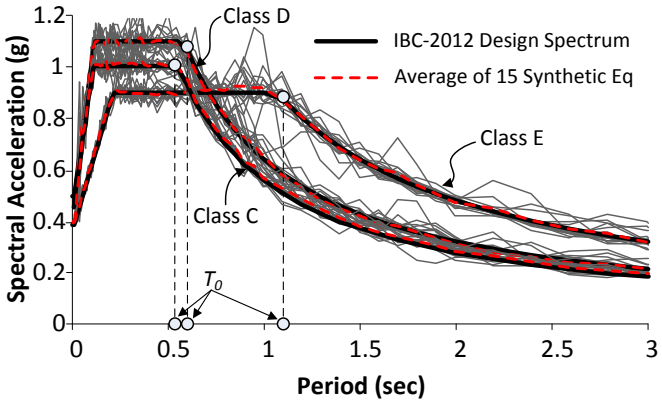

Fig. 3. Comparison of mean response spectra of 15 synthetic earthquakes with IBC-2012 code response spectra for site classes C, D and E

Table 3. Site soil classifications according to IBC-2012.

Site class	Soil profile name	$V_{s,30}$ (m/s)	T_0 (sec)	ν
A	Hard rock	>1500	N/A	N/A
B	Rock	760-1500	N/A	N/A
C	Very dense soil/soft rock	360-760	0.56	0.33
D	stiff soil	180-360	0.60	0.40
E	soft soil	<180	1.10	0.50

2.3 Modelling Parameters and General Procedures

The overall dynamic response of a soil-structure system is dependent on the properties of the structure compared to those of the soil. This interdependence can be described by using the following dimensionless parameters:

1. The structure-to-soil stiffness ratio a_0, which is defined as:

$$a_0 = \frac{\omega_n \overline{H}}{V_s} \tag{6}$$

where $\omega_n=2\pi/T_n$ is the circular frequency of the fixed-base structure corresponding to its first mode of vibration; $\overline{H}$ is the effective height of the structure that can be approximated as 0.7 times the total height of the structure h_{tot}, according to the ATC-40 provisions [26]; and $V_s= V_{s,30}$ is the average shear wave velocity of the top 30 meters of the soil deposit.

2. The slenderness ratio of the structure s, which is given by:

$$s = \frac{\overline{H}}{r} \tag{7}$$

3. The structure-to-soil mass ratio $\overline{m}$:

$$\overline{m} = \frac{m_{tot}}{\rho h_{tot} r^2} \tag{8}$$

which is set equal to 0.5 for common buildings [11].

It can be noted that the structure-to-soil stiffness ratio a_0, which measures the stiffness of the structure relative to that of the underlying soil, is a function of V_s , which is also used to classify soil sites in most current seismic codes (see Table 3). Fig. 4 illustrates the practical range of a_0 for various types of multi-storey buildings located on different site classes according to IBC-2012 [28]. The results

are presented as a_0 versus $V_{s,30}$ on a log-log scale, while the fundamental period of each structural system is estimated based on Eq. (5). To cover a wide range of SSI conditions, the abscissa in Fig. 4 starts at 90 m/s representing the average value of site class E, and ends at 1500 m/s which represents a fixed-base condition for common buildings located on site class A. It is seen from Fig. 4 that, for a given shear wave velocity, a greater a_0 value is always expected for tall buildings. While the maximum value of a_0 for frame structures is about 2, it is shown that a_0 can increase to up to 3 for other structural systems. Previous studies demonstrated that the effect of SSI on the seismic performance of common structures is usually negligible when a_0<0.5 (e.g. [33]). Therefore, this study will mainly focus on a_0 values of 0, 1, 2 and 3 and site classes C, D and E (i.e. very dense to soft soil).

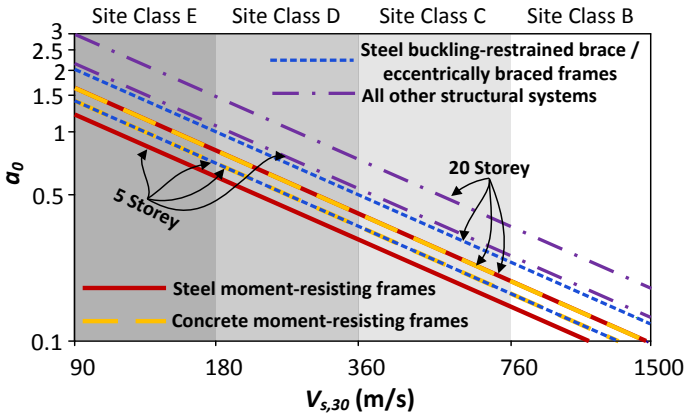

Fig. 4. Practical range of a_0 for various types of structures located on different soil sites according to IBC-2012 [28].

To investigate the influence of each design parameter on the seismic response of SSI systems, 1, 5, 10, 15 and 20-storey shear-building models with s=1, 2, 3 and 4 were subjected to the code spectrum-compatible synthetic earthquakes, considering four levels of inelasticity μ=2, 4, 6 and 8. The mean response of the structures was obtained by averaging the results for each set of synthetic records representing a specific site-class. For shallow foundations subjected to horizontal motions of a vertically propagating shear wave, kinematic interactions can reasonably be ignored [34]. As a result, the ground motions were directly applied to the foundation. It should be emphasised that while the range of some design parameters investigated in this paper may be much wider than their practical values, they are used for comparison purposes. Only the practical design values shown in Fig. 4 were used to develop the design methodology for flexible-base structures in this study.

The authors developed a programme in MATLAB [35] to conduct nonlinear dynamic analyses of MDOF SSI systems. The results were obtained in the time domain using the Newmark's time-stepping method [36]. In order to solve the nonlinear equations, the modified Newton-Raphson's iterative scheme was utilised. A large number of verification analyses were performed to prove the validity of the models using various methods. The nonlinear dynamic response of the flexibly-supported structures was calculated over a wide range of fixed-base fundamental periods from 0.1 to 3 sec. The general procedure for the development of the SSI models and the calculation of the strength demands is illustrated in Fig. 5. For each storey in a given simulation, the peak storey ductility ratio was calculated as the maximum shear deformation divided by the yield deformation. The maximum value of the peak storey ductility ratios was used as the ductility demand of an MDOF building, as done by Santa-Ana and Miranda [13], Moghaddam and Mohammadi [37], and Ganjavi and Hao [38]. It should be mentioned that this ductility demand excludes the effects of the rigid body movements caused by the translation and rotation of the foundation and, therefore, can directly reflect the expected damage of the superstructure. In shear building structures, any increase in structural material is normally accompanied by an increase in storey strength and, therefore, total structural weight could be considered proportional to the sum of all storey shear strengths [20]. In this study, an iterative method was used to calculate appropriate strength demands F_{tot} (defined as the sum of the storey strengths) for the SSI systems to achieve a prescribed ductility μ_t, while maintaining the initial pattern of the strength distribution. It should be noted that storey ductility does not increase monotonically when reducing the strength [9], which means that there could be more than one strength satisfying a given ductility. In this case, only the highest strength was considered [39].

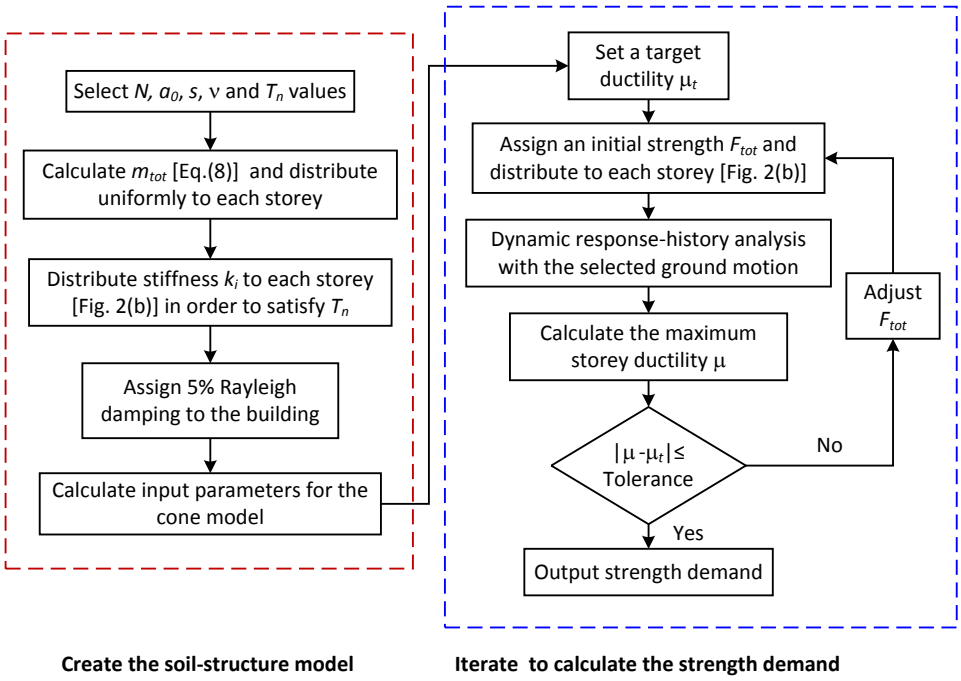

Fig. 5. Flowchart showing the general procedure for evaluation of strength demands of flexible-base MDOF buildings.

3 Strength Demands of MDOF SSI Systems

In this section, the effects of lateral seismic design load pattern, structure-to-soil stiffness ratio, structural slenderness and site conditions on the strength-ductility relationship of multi-storey flexible-base buildings are investigated.

3.1 Effects of Design Lateral Load Pattern

The lateral seismic design load pattern can significantly influence the stiffness and strength distributions in multi-storey buildings, and hence the displacement and strength demands under seismic excitations. Fig. 6 compares the total strength demand F_{tot} of fixed-base (a_0=0) and flexible-base (a_0=3) 10-storey buildings (s=2) designed with different load patterns. Again, F_{tot} was calculated by summing the strength demands of all storeys. It is clear from Fig. 4 that for a typical 10-storey building (a_0 values between 5 and 20-storey limits), a_0=3 corresponds to a soil condition of site class E. Therefore, the results in Fig. 6 are the average values from the fifteen spectrum-compatible earthquakes corresponding to Class E. Results for other slenderness ratios and site classes showed similar trends to those presented in Fig. 6. For better comparison, the strength demands are normalised by the product of the total mass of the structure and PGA. The shaded areas on the graphs in Fig. 6 represent the practical range of the fundamental period of a 10-storey building with different structural systems calculated using Eq. (5).

Fig. 6 shows that the strength demands of the buildings designed according to the concentric and rectangular load patterns are always higher than those corresponding to the other load patterns, especially for lower values of fundamental period. Within the practical range of the fundamental period of a typical 10-storey building (i.e. shaded areas), using the concentric and rectangular load distributions can result in up to 1.68 and 2 times higher strength demands, respectively, compared to code-based load patterns such as IBC-2012 and Eurocode 8. It should be mentioned that this observation is opposite to conclusions made by Ganjavi and Hao [38], where the concentric pattern was found to yield the lowest strength demand. The reason for this difference is attributed to different definitions of strength demand used in the two studies. The current study calculated the total strength as the sum of all storey strengths, whereas Ganjavi and Hao used the base shear strength that corresponds only to the strength of the first storey. The total strength demand that is used in the current study can be considered proportional to the total structural weight of the shear building [30] and is, therefore, a more appropriate parameter to compare the seismic performance of buildings designed according to different lateral load patterns.

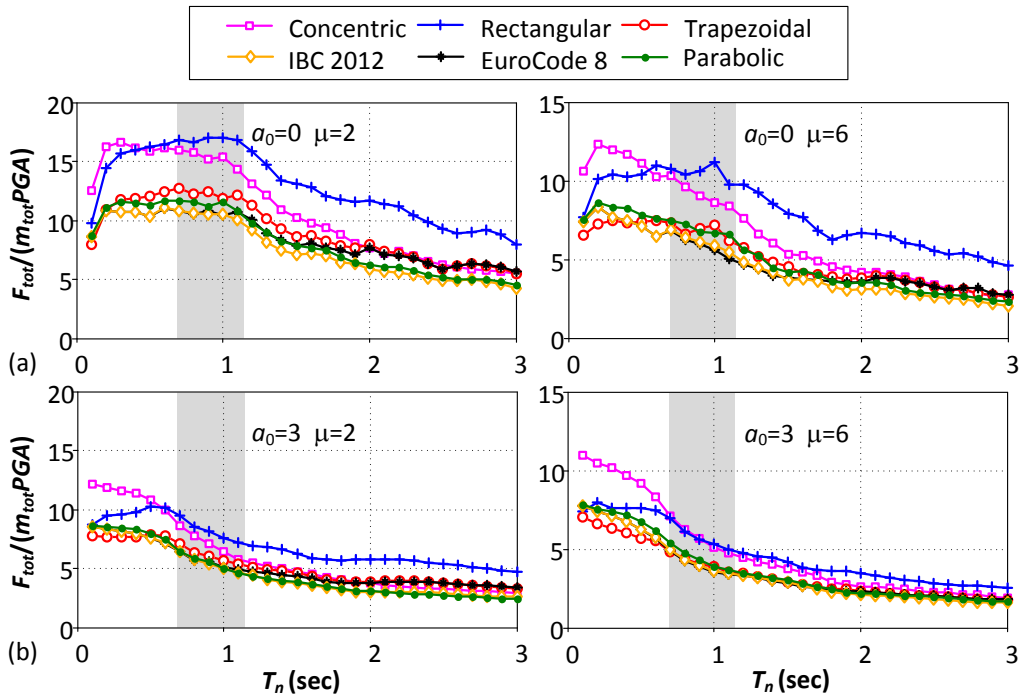

Fig. 6. Total strength demands of (a) fixed-base and (b) flexible-base 10-storey buildings designed according to different lateral load patterns, Soil Class E, s=2.

Although strength demands corresponding to parabolic, trapezoidal and code-based load patterns are not significantly different, especially for the SSI systems, the trapezoidal lateral load pattern is in general the most suitable for seismic design of nonlinear short period flexible-base structures (i.e. requires minimum total strength to satisfy a target ductility demand) and code-specified design patterns are more appropriate for structures with a fundamental period T_n>0.8 sec. This conclusion is in agreement with the results reported by Moghaddam and Hajirasouliha [40] for fixed-base shear-buildings subjected to a group of natural earthquake excitations.

Based on the concept of uniform damage distribution, it can be assumed that the uniform distribution of deformation demands is a direct consequence of the optimum use of material [30]. Therefore, the coefficient of variation of storey ductility demands (COV_μ) can be used as a performance parameter to evaluate the effectiveness of different lateral load patterns. Fig. 7 compares the mean COV_μ of fixed-base and SSI systems designed according to different load patterns under fifteen spectrum-compatible earthquakes corresponding to site class E. As expected, the concentric and rectangular patterns resulted in a much higher COV_μ compared to other load patterns. Within the expected range of periods for 10-storey frames (i.e. shaded areas), the concentric pattern always led to the largest ductility dispersion, while the code patterns provided the best design solutions.

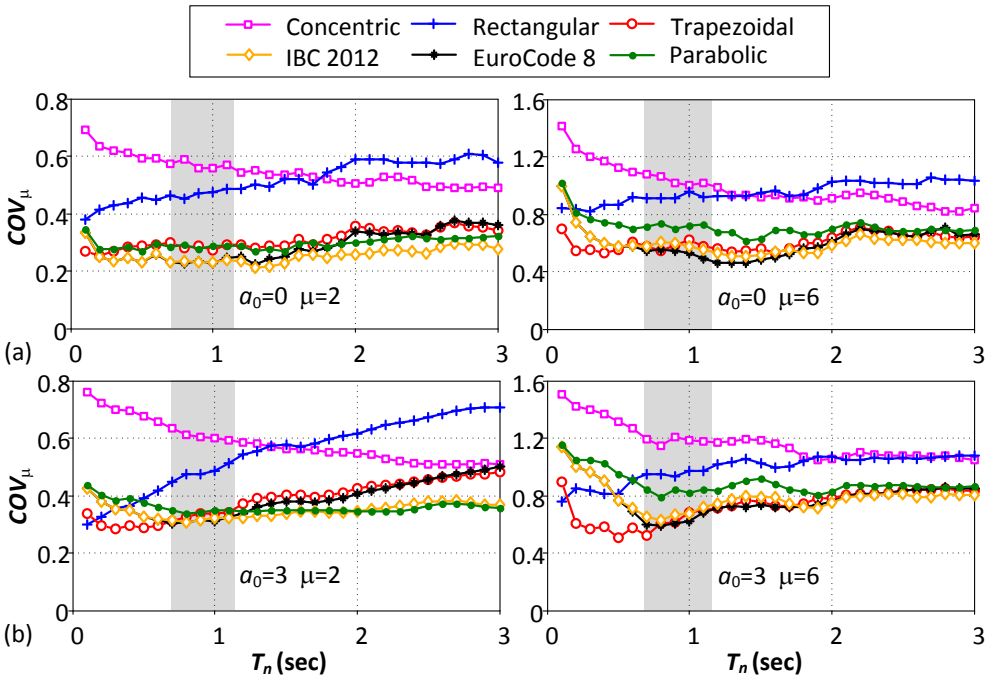

Fig. 7. Coefficient of variation of storey ductility for (a) fixed-base and (b) flexible-base 10-storey buildings designed according to different lateral load patterns, Soil Class E, s=2.

3.2 Effects of Structure to Soil Stiffness Ratio and Slenderness Ratio

Fig. 8 compares the total strength demands of 10-storey buildings, designed according to IBC-2012 load pattern, with fundamental periods ranging from 0.1 to 3 sec and target ductility demands μ=2 and 8 for structure-to-soil stiffness ratios a_0=0, 1, 2 and 3 (720 models in total). The shaded areas represent the expected periods of typical 10-storey frames according to ASCE 7-10 [31]. It should be noted that the selected ranges of the design parameters are only for comparison purposes; some cases do not represent practical scenarios. For example, as discussed in Section 2.3, a value of 3 for a_0 is not suitable for common buildings located on soil site class C (see Fig. 4).

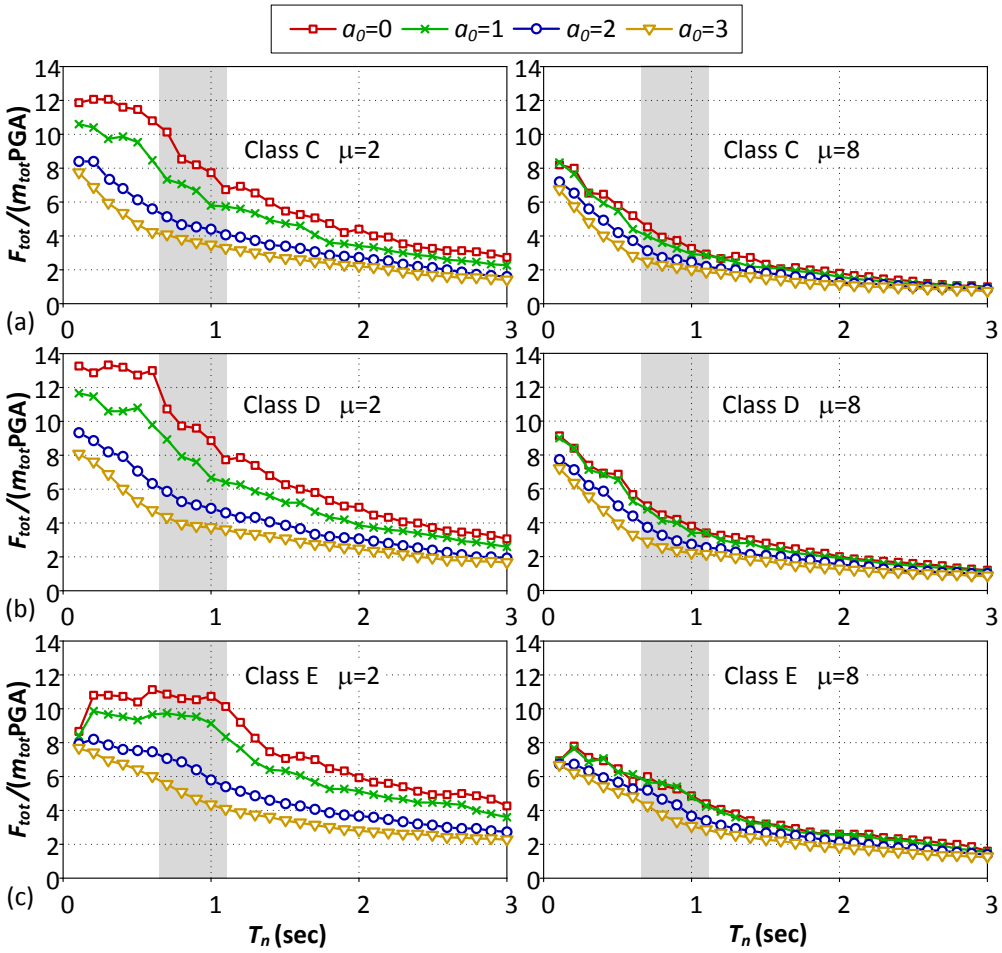

Fig. 8. Total strength demands of 10-storey structures (s=1) located on (a) class C, (b) class D and (c) class E for μ=2 and 8.

Overall, the results shown in Fig. 8 indicate that increasing structure-to-soil stiffness ratio a_0 reduces the structural strength demands of SSI systems in comparison to their fixed-base counterparts, especially for lightly nonlinear systems. For instance, Fig. 8(c) shows that for a flexible-base building

with a fixed-base fundamental period of 1 sec, s=1, and a_0=3, the total strength demand is reduced by 60% compared to the situation without SSI (i.e. a_0=0). This implies that considering SSI in the seismic design of typical multi-storey buildings can lead to more cost-effective design solutions with less structural weight. This beneficial effect, however, becomes less prominent for highly nonlinear structures and the difference between the results of fixed-base and flexible-base systems becomes less significant when structures undergo large inelastic deformations (i.e. μ>8). This observation is consistent with that made by Veletsos and Verbic [41] and Ghannad and Jahankhah [11], which can be explained by the fact that the energy dissipated by the soil medium would be negligible compared to that caused by plastic deformations of highly nonlinear structures.

The effect of slenderness ratio on total strength demand of MDOF SSI systems is investigated in Fig. 9 for 10-storey buildings designed according to the IBC-2012 design load pattern. It is shown that, in general, slenderness ratio does not significantly affect the strength demands of inelastic systems, especially in the high period region (i.e. T_n>1sec). This effect is further reduced by increasing structural inelasticity level μ or by reducing the structural stiffness relative to that of the soil a_0. On the contrary, for lightly nonlinear systems with high a_0 values (e.g. a_0=3, μ=2), the structures designed with s=1 exhibit a lower total strength demand than those with higher slenderness ratio (s=2, 3 and 4), especially in the low period range. Previous studies showed that SSI systems with s=1 have a much higher effective damping ratio than those with greater slenderness ratios (e.g. s=2, 3 and 4), which is more pronounced in structures with higher structure-to-soil stiffness ratio a_0 [23, 42]. Therefore, it is suggested that the difference caused by slenderness ratio in the total structural strength demands is mainly attributed to the effective damping of the SSI system ξ_{ssi}, which increases as the slenderness ratio is reduced. The effective damping, however, makes a small contribution to the total energy dissipation when compared with that provided by large inelastic deformations, as described previously.

4 SDOF DUCTILITY REDUCTION FACTOR, R_μ

The ductility reduction factor R_μ for an SDOF system is generally defined as the ratio of the elastic to inelastic base shear corresponding to a target ductility demand. Based on this definition, the following equation can be used to calculate R_μ for an SDOF SSI system:

$$R_{\mu} = \frac{V_{SDOF}(T_n, a_0, s, \mu = 1)}{V_{SDOF}(T_n, a_0, s, \mu = \mu_t)} \tag{9}$$

where $V_{SDOF}(T_n,a_0,s,\mu=1)$ and $V_{SDOF}(T_n,a_0,s,\mu=\mu_t)$ are the required base shear demands for an SDOF structure to remain elastic and to achieve a target ductility of μ_t, respectively. Note that a_0=0 corresponds to a fixed-base condition, whereas a_0>0 represents an SSI condition. The ductility reduction factor R_μ in Eq. (9) only relates to a strength reduction due to the inelastic hysteretic behaviour of the structure and, therefore, can be used for both fixed-base and flexible-base buildings.

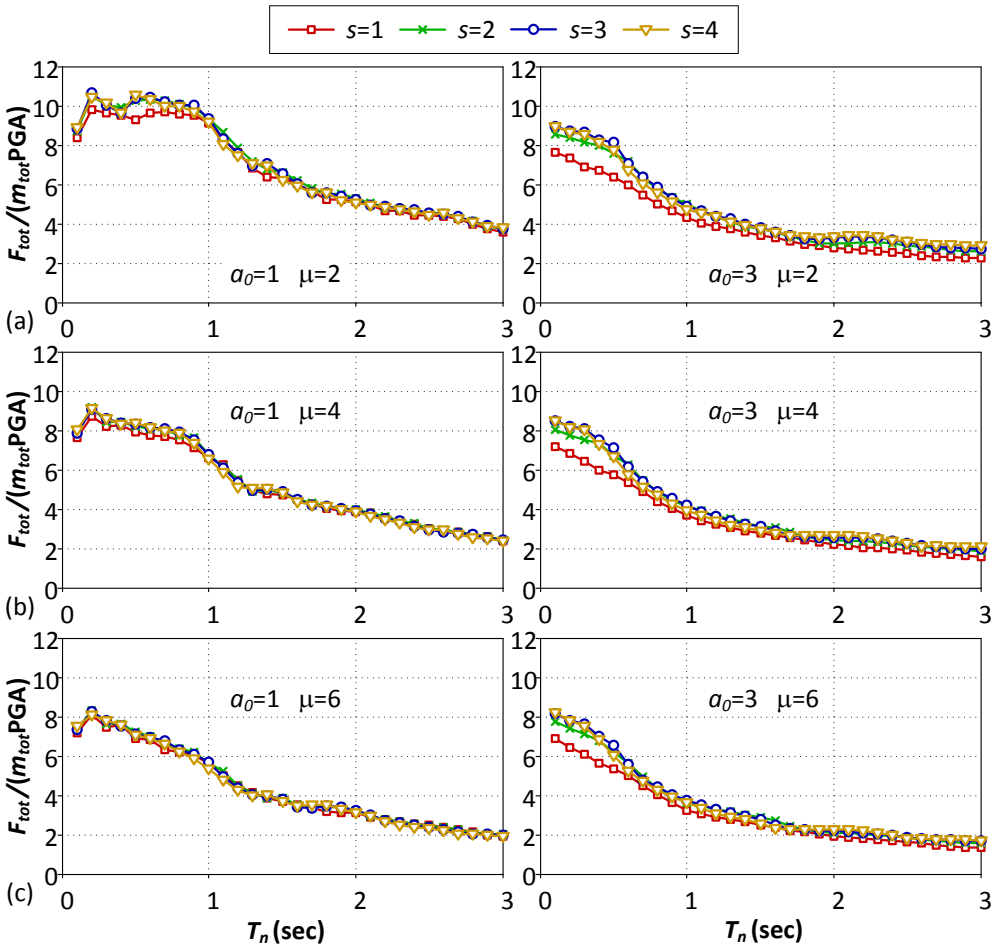

Fig. 9. Effect of slenderness ratio on total strength demands of 10-storey SSI systems on soil site class E for (a) μ=2, (b) μ=4 and (c) μ=6.

Fig. 10 compares the ductility reduction factor of SDOF systems for different site classes considering various combinations of a_0, s and μ. Results are averaged values for 15 synthetic spectrum-compatible earthquakes corresponding to each site class. Generally, an ascending trend is observed for R_μ when increasing the fixed-base natural period T_n, especially in the low period range. This trend,

however, is less pronounced in the high period region. For the rigid-base systems (i.e. a_0=0), the R_μ curves show two distinct segments that are separated by a transition point at a threshold period. The first segment corresponds to a monotonically increasing R_μ with T_n, whereas the second segment exhibits an oscillating R_μ around a maximum value, which is much less affected by T_n. This observation can be well described by a bi-linear approximation of R_μ versus T_n proposed by Vidic et al. [43], with the threshold period almost equal to the characteristic period T_0.

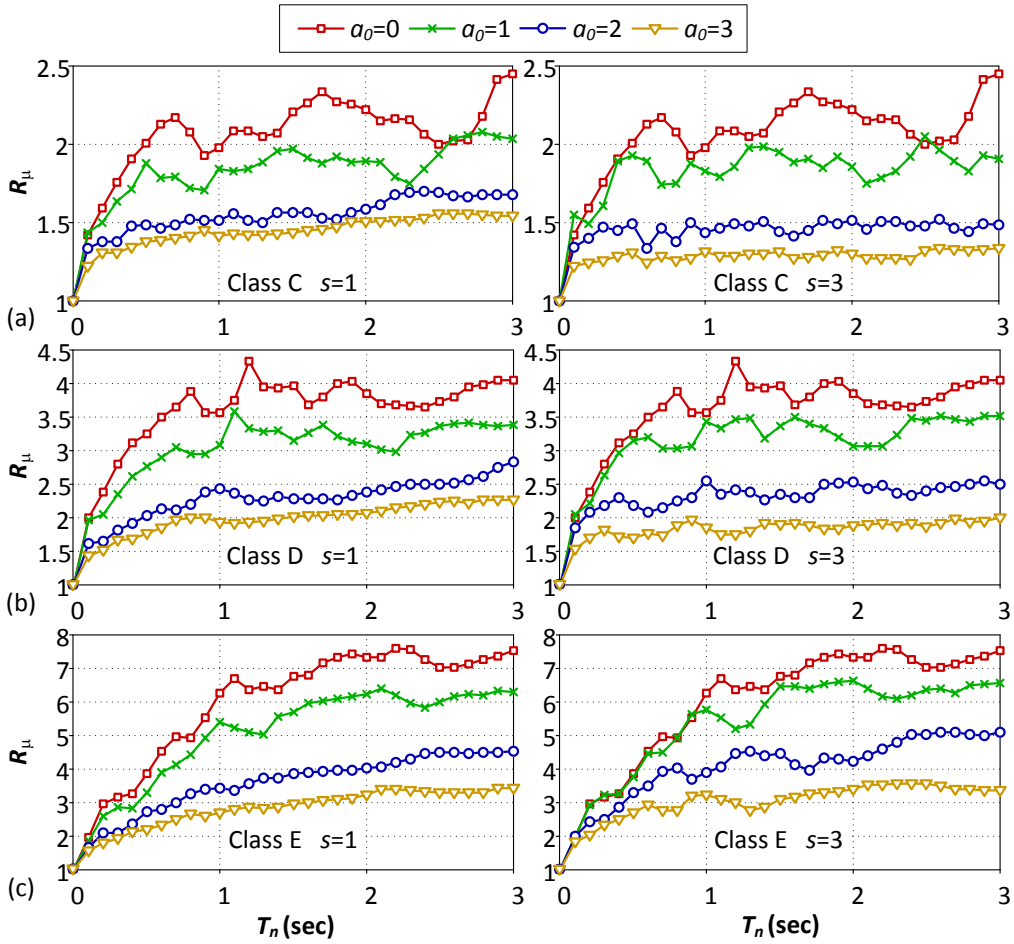

Fig. 10. Effect of SSI on ductility reduction factor R_μ of SDOF structures located on different site classes considering three levels of ductility demands (a) μ=2, (b) μ=4 and (c) μ=8.

For flexible-base systems shown in Fig. 10, the bi-linear approximation of R_μ spectra seems to provide reasonable results, but the threshold periods are considerably lower than T_0, especially for systems with greater a_0 values and higher slenderness ratios. This could be a result of period lengthening due to SSI, which causes the transition points to occur earlier in the spectra. It is observed that the ductility reduction factor R_μ decreases by increasing the a_0 value, which was also reported by

Ghannad and Jahankhah [11], who concluded that using a fixed-base reduction factor to design a flexibly-supported structure is un-conservative.

It should be noted that applying conventional R_μ-T_n relationships for seismic design of flexible-base structures may not be appropriate, since the slenderness ratio can lead to inconsistent results in R_μ spectra. For example, a higher slenderness ratio can either result in a larger (Fig. 10(c)) or a smaller (Fig. 10(a, b)) R_μ factor for SSI systems with a_0=2 and 3 in the long period range. This inconsistency can be addressed by presenting the ductility reduction factor in a R_μ versus T_{ssi} format, where T_{ssi} is the elongated period of an SSI system that can be calculated according to Maravas et al. [42]. Moreover, it was shown in Fig. 8 that the fixed-base and SSI systems practically lead to similar results for highly nonlinear structures. This is further verified in Fig. 11, which compares the mean base shear demand of SDOF systems with and without considering SSI effects. It is observed that the SSI effect can considerably reduce (up to 50 %) the base shear demands of lightly-nonlinear systems (i.e. μ=2), while it is almost negligible for highly-nonlinear systems (i.e. μ=8). It can also be noted that, in the short period range, flexible-base SDOF structures may experience a lager base shear than their fixed-base counterparts for the same level of ductility demand (see Fig. 11(b)). This can be explained by the fact that the effective damping ratio of an SSI system could be less than that of the structure in its fixed-base condition, especially for those having a higher slenderness ratio [23, 42].

In an analogy to R_μ for SDOF systems, Ganjavi and Hao [14, 38] proposed that the base shear demand of nonlinear MDOF systems can be estimated from the base shear demand of their elastic counterparts through a ductility reduction factor given by:

$$R_{\mu,MDOF} = \frac{V_{MDOF}\left(T_n, a_0, s, \mu_{\max} = 1\right)}{V_{MDOF}\left(T_n, a_0, s, \mu_{\max} = \mu_t\right)} \tag{10}$$

where $V_{MDOF}(T_n,a_0,s,\mu_{max}=\mu_t)$ is the base shear strength of an MDOF structure to avoid the maximum storey ductility μ_{max} exceeding the target value μ_t and $V_{MDOF}(T_n,a_0,s,\mu_{max}=1)$ is the base shear strength demand of an MDOF system to remain elastic during the design earthquake. It should be noted that, considering the frequency dependence of the foundation stiffness in SSI systems, calculation of

$V_{MDOF}(T_n,a_0,s,\mu_{max}=1)$ could be difficult for flexible-base MDOF structures and, therefore, Eq. (10) cannot be directly used in the seismic design process.

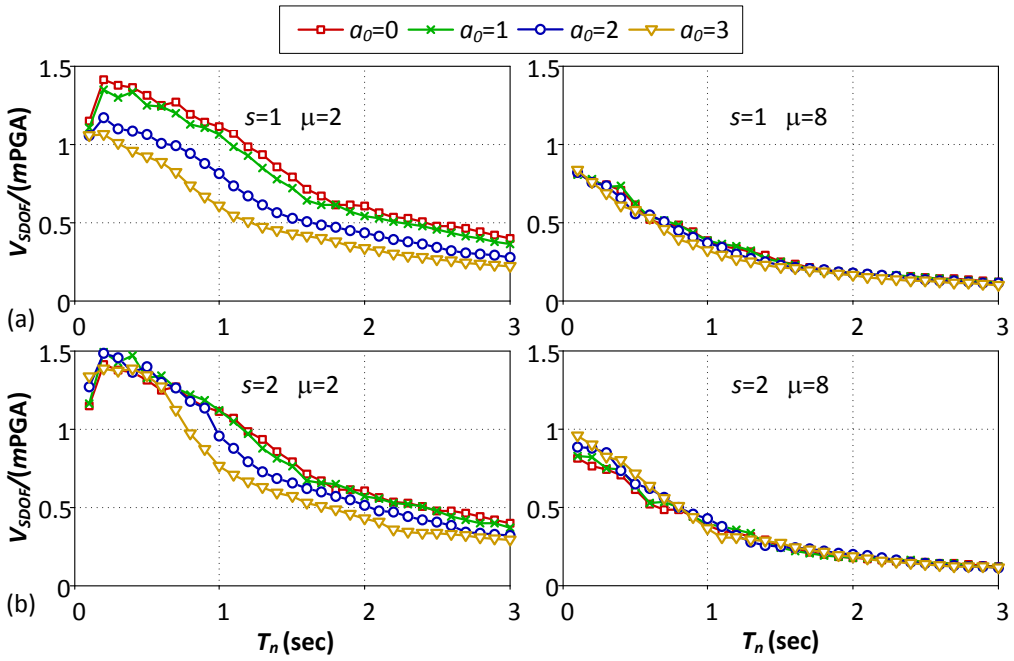

Fig. 11. Base shear demands of SDOF structures located on site class E.

In view of addressing the above mentioned issues, section 5 presents a new strength reduction factor R_F for SDOF systems based on a definition that is more suitable for performance-based seismic design of flexible-base structures, while in section 6 a site and interaction-dependent MDOF modification factor R_M is introduced to account for the MDOF effects in SSI systems.

5 SDOF STRENGTH REDUCTION FACTOR, R_F

Based on the above discussion, a more practical strength reduction factor definition R_F is suggested in this study to use fixed-base SDOF elastic design spectra (e.g. from seismic design guidelines) for seismic design of nonlinear MDOF SSI systems.

$$R_F = \frac{V_{SDOF}(T_n, a_0 = 0, \mu = 1)}{V_{SDOF}(T_n, a_0, s, \mu = \mu_t)} \tag{11}$$

Note that if a_0=0, R_F corresponds to R_μ for fixed-base structures (whose dynamic responses are not affected by s), which reflects the reduction only attributed to the nonlinear behaviour of the structures; while μ_t=1 leads to a R_μ associated with the reduction only due to the SSI effects (i.e. inelastic hysteretic behaviour of structures is excluded). Therefore, R_F defined in Eq. (11) can be interpreted as a

strength reduction factor due to the combination of yielding and SSI effects. In this study, based on the results of more than 100,000 dynamic analyses of 7200 SDOF systems, the following equation is proposed to estimate the strength reduction factor R_F:

$$\begin{cases} R_F = \dfrac{R-1}{T_0}T + 1, & for \quad 0 \le T \le T_0 \\ R_F = R, & for \quad T \ge T_0 \end{cases} \tag{12}$$

where R is a function of ductility demand μ, structure-to-soil stiffness ratio a_0, and slenderness ratio s, with its values presented in Table 4. T_0 is the characteristic period of the design ground motions as shown in Fig. 3. The shape of R_F spectra described by Eq. (12) was originally proposed by Vidic et al. [43] for design of inelastic fixed-base structures.

Table 4. Proposed values for R in Eq. (12)

R	a_0=0				a_0=1				a_0=2				a_0=3			
	s=1	s=2	s=3	s=4	s=1	s=2	s=3	s=4	s=1	s=2	s=3	s=4	s=1	s=2	s=3	s=4
Soil class C																
μ=1	1.0	1.0	1.0	1.0	1.3	1.2	1.2	1.2	2.0	1.7	1.7	1.7	2.8	2.4	2.3	2.3
μ=2	2.2	2.2	2.2	2.2	2.4	2.2	2.2	2.1	3.2	2.6	2.4	2.5	4.1	3.2	2.9	3.0
μ=4	3.9	3.9	3.9	3.9	4.1	3.9	3.9	3.9	4.8	4.2	3.9	3.9	5.6	4.5	4.2	4.1
μ=6	5.4	5.4	5.4	5.4	5.5	5.4	5.3	5.3	6.1	5.6	5.4	5.3	7.0	5.8	5.3	5.2
μ=8	6.8	6.8	6.8	6.8	6.8	6.7	6.7	6.7	7.4	6.8	6.7	6.6	8.2	7.1	6.5	6.2
Soil class D																
μ=1	1.0	1.0	1.0	1.0	1.2	1.1	1.1	1.1	1.9	1.6	1.6	1.6	2.7	2.3	2.2	2.2
μ=2	2.1	2.1	2.1	2.1	2.3	2.3	2.1	2.1	3.0	2.5	2.4	2.4	3.9	3.1	2.8	2.8
μ=4	3.8	3.8	3.8	3.8	3.9	3.8	3.7	3.7	4.6	4.0	3.8	3.7	5.5	4.4	4.0	4.0
μ=6	5.3	5.3	5.3	5.3	5.3	5.2	5.2	5.2	5.9	5.4	5.2	5.1	6.8	5.7	5.2	5.0
μ=8	6.6	6.6	6.6	6.6	6.6	6.5	6.5	6.5	7.2	6.7	6.5	6.3	8.0	6.9	6.5	6.2
Soil class E																
μ=1	1.0	1.0	1.0	1.0	1.2	1.1	1.1	1.1	1.9	1.6	1.5	1.6	2.7	2.2	2.1	2.1
μ=2	2.2	2.2	2.2	2.2	2.4	2.3	2.2	2.2	3.1	2.6	2.4	2.4	4.0	3.0	2.8	2.8
μ=4	4.1	4.1	4.1	4.1	4.1	4.0	4.0	4.0	4.7	4.2	4.0	4.0	5.6	4.5	4.2	4.1
μ=6	5.7	5.7	5.7	5.7	5.7	5.6	5.5	5.5	6.2	5.7	5.5	5.5	7.0	6.0	5.5	5.4
μ=8	7.1	7.1	7.1	7.1	7.1	7.0	7.0	6.9	7.5	7.0	6.9	6.8	8.2	7.2	6.8	6.5
Average																
μ=1	1.0	1.0	1.0	1.0	1.2	1.1	1.1	1.1	2.0	1.6	1.6	1.6	2.7	2.3	2.2	2.2
μ=2	2.2	2.2	2.2	2.2	2.4	2.3	2.2	2.1	3.1	2.6	2.4	2.4	4.0	3.1	2.8	2.9
μ=4	3.9	3.9	3.9	3.9	4.0	3.9	3.9	3.9	4.7	4.1	3.9	3.9	5.6	4.5	4.1	4.1
μ=6	5.5	5.5	5.5	5.5	5.5	5.4	5.3	5.3	6.1	5.6	5.4	5.3	6.9	5.8	5.3	5.2
μ=8	6.8	6.8	6.8	6.8	6.8	6.7	6.7	6.7	7.4	6.8	6.7	6.6	8.1	7.1	6.6	6.3

Fig. 12 compares the mean values of strength reduction factor R_F for SDOF SSI systems obtained from response-history analyses with those calculated according to Eq. (12). It is shown that the R_F versus T_n curves follow reasonably closely a bi-linear relationship with the intersection of two linear segments approximately corresponding to the characteristic periods of the design spectrum T_0 for each site class. Regression analyses were done to obtain best-fit values for R in Eq. (12), which minimised the sum of the squared residuals over all period points. The residual is defined as the difference between the mean value of R_F and that calculated by Eq. (12) at a period T_n.

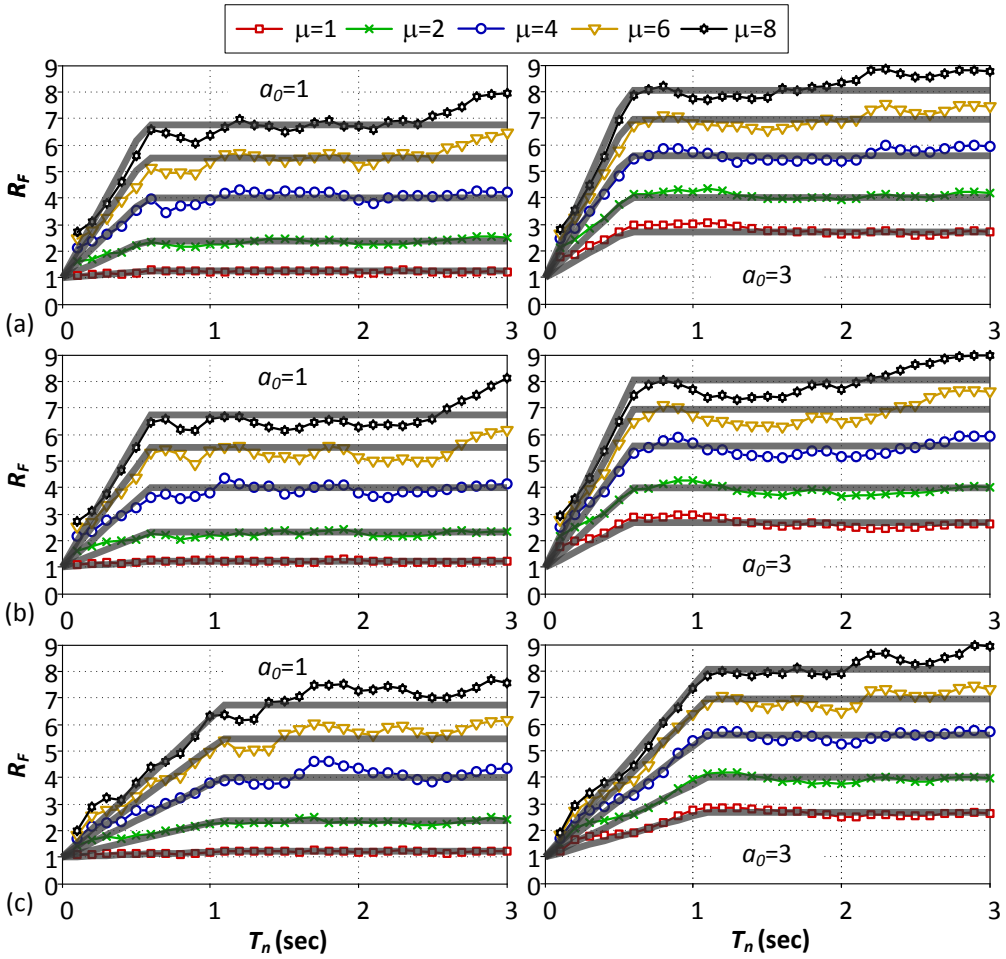

Fig. 12. Comparison of the mean strength reduction factors R_F with those calculated using Eq. (12) (bi-linear lines) for SDOF SSI systems (s=1) on (a) site class C, (b) site class D, and (c) site class E.

Table 4 shows that the R values, in general, are not sensitive to the soil site classes, especially for lower ductility demands. Therefore, it is suggested that the average R values presented in Table 4, which are site-independent, may be used in Eq. (12). As expected, the results indicate that the

slenderness ratio of the structure, s, has a negligible effect on R values when the structure-to-soil stiffness ratio a_0 is small (i.e. a_0<1), and hence the SSI effects are not dominant.

The proposed equation for strength reduction factor R_F not only addresses the issues associated with the conventional R_μ-T_n relationships discussed in Section 4, but also has two prominent advantages. Firstly, it captures the reduction of strength due to the combination of SSI and structural yielding, with the SSI effect being negligible for structures with high ductility demands. Secondly, the inelastic strength demand of a flexible-base structure can be directly estimated from the elastic response of its corresponding fixed-base structure through the reduction factor R_F. This implies that by using Eq. (12), the calculation of the base shear demand of flexible-base structures does not require the knowledge of the elastic response spectra derived for SSI systems, which is ideal for practical design purposes.

6 MDOF MODIFICATION FACTOR (R_M) of SSI Systems

In order to use an SDOF design spectrum for MDOF systems, modifications should be made to take into account the higher mode effects. Considering SDOF and MDOF structures with similar mass m and fundamental period T_n, the MDOF modification factor for a flexible-base structure can be defined as:

$$R_M = \frac{V_{SDOF}\left(T_n, a_0, s, \mu = \mu_t\right)}{V_{MDOF}\left(T_n, a_0, s, \mu_{\max} = \mu_t\right)} \tag{13}$$

where $V_{MDOF}(T_n,a_0,s,\mu_{max}=\mu_t)$ is the base shear strength for an MDOF structure to avoid the maximum storey ductility μ_{max} exceeding the target value μ_t. Note that when a_0=0, Eq. (13) is an expression for the fixed-base MDOF modification factor, which was proposed by Nassar and Krawinkler [44] and has received much attention in the past two decades [13, 37, 45].

The base shear strength demand of an inelastic flexible-base MDOF system can be determined from the elastic spectrum for an equivalent fixed-base SDOF system by using Eqs. (11) and (13), as follows:

$$V_{MDOF}(T_n, a_0, s, \mu_{\max} = \mu_t) = \frac{V_{SDOF}(T_n, a_0 = 0, \mu = 1)}{R_F R_M} \tag{14}$$

In this study, 5, 10, 15 and 20-storey shear buildings are utilised to obtain the MDOF modification factor R_M for SSI systems, considering various structural types and soil site classes. The buildings are assumed to be symmetric and represent typical 5-bay structures having a span length of 6 meters. Using

a storey height of 3.3 meters, the slenderness ratios corresponding to 5, 10, 15 and 20-storey buildings would be approximately 0.7, 1.4, 2 and 2.7, respectively. The effective foundation radii for swaying and rocking modes were calculated based on equating the area A_f and moment of inertia I_f of each floor to those of an equivalent circle (i.e. $r_h = \sqrt{A_f / \pi}$ and $r_\theta = \sqrt[4]{4I_f / \pi}$). The fundamental period of the buildings was determined according to Eq. (5) for the four different ASCE 7-10 [31] structural types listed in Table 2.

In order to derive a site dependent R_M, an averaged shear wave velocity was used to represent each site soil condition, that is $V_{s,30}$=90, 270 and 560m/s for site classes E, D and C, respectively. Therefore, the corresponding a_0 value for an MDOF structure located on a specific soil deposit could be estimated from Fig. 4. The range of expected a_0 values for different SSI systems is presented in Fig. 13, which shows higher a_0 values for taller buildings and softer soil conditions. It is observed that frame structures (i.e. type 1-3) have a lower a_0 value compared with other structural systems (i.e. type 4), especially for those located on site class E. Therefore, for better comparison, frame structures are presented as one group in Fig. 13. It can be noted that the expected a_0 values for typical buildings founded on site class C (average shear wave velocity of 560 m/s) are close to zero. This implies that the seismic design of typical multi-storey buildings on site classes A, B and even C (see Table 3) could be practically done on the basis of fixed-base structures.

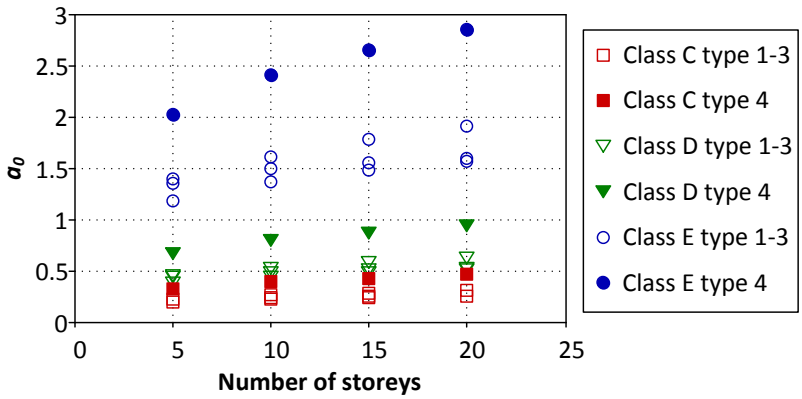

Fig. 13. Variation of a_0 with number of storeys for different types of structural systems on various site classes.

The effect of using different structural types (types 1 to 4 in Table 2) on $1/R_M$ is presented in Fig. 14. It should be noted that shear buildings, in general, cannot accurately represent all different structural

systems and, therefore, the effect of "structural type" in this context is attributed mostly to the expected fundamental period of the structures using Eq. (5). As mentioned previously, according to ASCE 7-10 [31], the expected fundamental period of frame structures (types 1-3) is much higher than type 4 structures. Therefore, the results in Fig. 14 illustrate lower $1/R_M$ values for type 4 structures compared to type 1-3 frame structures.

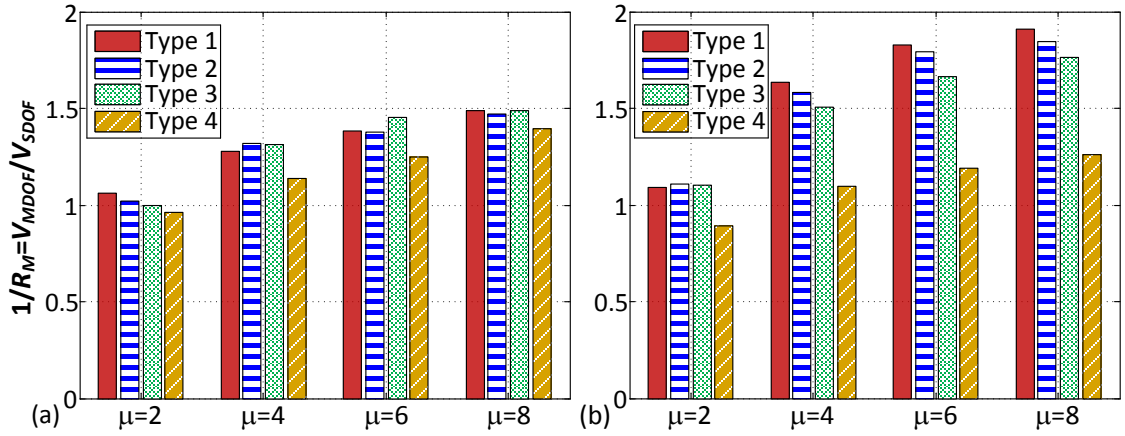

Fig. 14. Effect of structural type on MDOF modification factor for (a) 10-storey and (b) 15-storey structures located on Site class E.

Results for $1/R_M$ (averaged values for the 15 synthetic earthquakes in each set) are illustrated in Fig. 15, considering various structural types, numbers of storeys, ductility demands and site classes. Since the values of MDOF modification factor for frame structures are very close to each other (see Fig. 12), the results were averaged for structural types 1-3. As discussed previously, the effect of SSI is expected to be pronounced for site class E and insignificant for site class C.

Fig. 15 shows that, in general, inelastic MDOF structures require a higher base shear strength compared to their SDOF counterparts for the same target ductility demand, especially for tall buildings on stiff soil deposits. This observation is in agreement with findings presented by Santa-Ana and Miranda [13] for fixed-base structures. The results in Fig. 15 show a generally higher $1/R_M$ ($=V_{MDOF}/V_{SDOF}$) ratio for frame structures and stiff soil conditions than for other structural systems and soft soil profiles. $1/R_M$ curves also exhibit a general increasing trend with increasing ductility demand and number of storeys. Exceptions are observed for site class E where taller structures may have a lower value of $1/R_M$. As foundation soil becomes stiffer, the dependence of $1/R_M$ on ductility demand for moderately and highly nonlinear structures (μ=4, 6 and 8) is reduced. For example, the results for

site class C (very dense soil) in Fig. 15 show that the effect of ductility demand on $1/R_M$ for structures with μ=6 and 8 is practically negligible. This observation is consistent with the results reported by Moghaddam and Mohammadi [37], who investigated R_M for 5, 10 and 15-storey fixed-base MDOF shear buildings. In their study, R_M was found insensitive to ductility demand; a simple expression was suggested for estimating R_M as a function of number of storeys, as illustrated in Fig. 15 for soil class C (with minimum SSI effects). The fact that the R_M factor proposed by Moghaddam and Mohammadi [37] was derived through an averaging process for ductility values μ=2, 4, 6 and 8 is well reflected in this graph, since the results are generally bounded by the high and low-ductility limits used in this study.

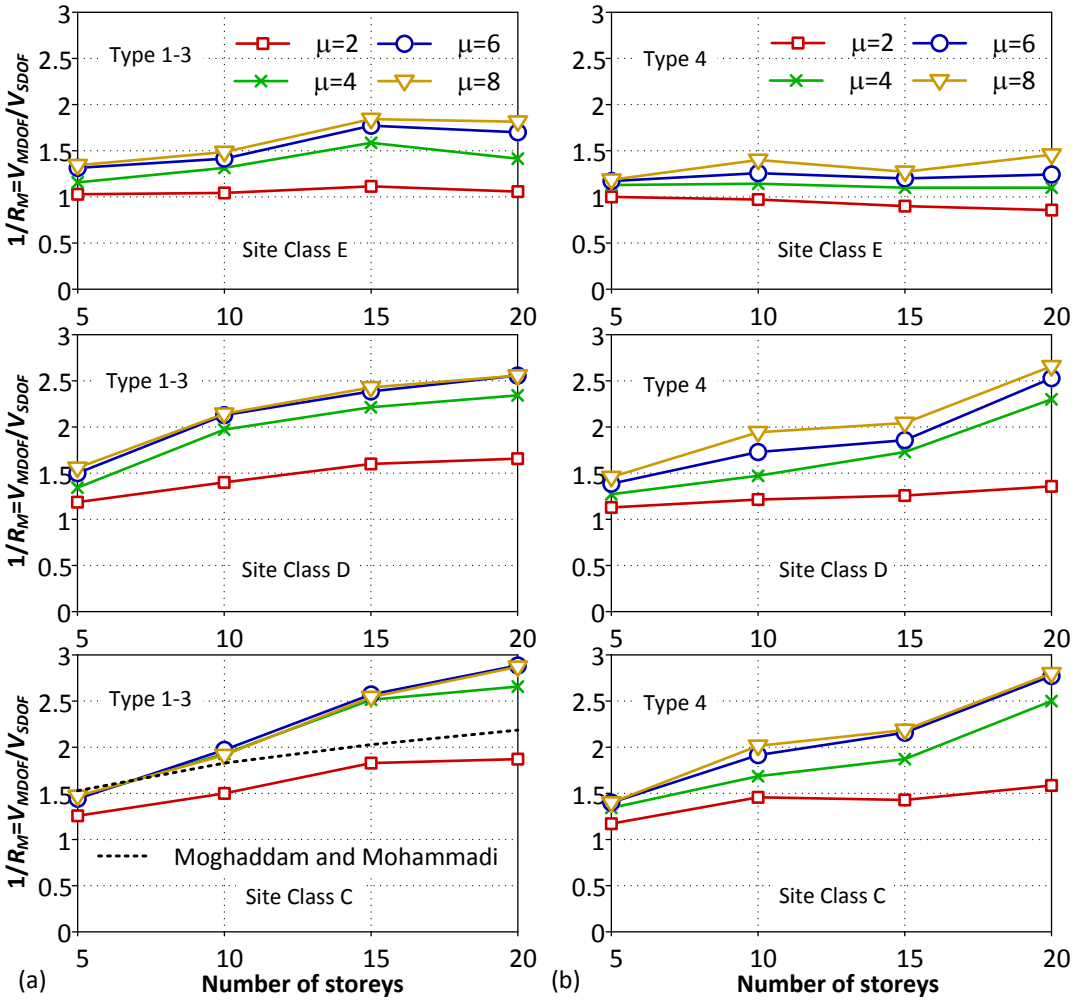

Fig. 15. Site and interaction-dependent MDOF-to-SDOF base shear strength ratio ($1/R_M$) for (a) frame structures and (b) all other types of structures.

The results of this study are used to develop a new practical site and interaction-dependent MDOF modification factor R_M for flexible-base structures. By assessing a variety of curves to obtain the best fit

to the results presented in Fig. 15, the following equation is suggested that is a function of number of storeys, ductility demand and site class:

$$\frac{1}{R_M} = 1 + (N-1)Ln(c\mu_t^{(0.05-N/1000)}) \quad (15)$$

where N is the number of storeys, μ_t is target ductility demand, and c is a soil dependent parameter that is equal to 1.040, 1.027 and 0.982 for site classes C, D and E, respectively. Although for elastic systems (i.e. μ_t=1) Eq. (15) suggests that base shear strengths of MDOF systems are equal to those of their corresponding SDOF systems, the results of this study indicate that for squat and stiff buildings (i.e. low fixed-base fundamental periods), the elastic base shear strengths of flexible-base MDOF structures are in general lower than those of their SDOF counterparts. However, for tall and very flexible buildings (i.e. very long fixed-base fundamental periods), the elastic base shear strengths of flexible-base MDOF structures can be much higher than their SDOF counterparts, especially for very soft soil conditions (i.e. higher values of a_0).

7 Performance-based Design Procedure

The proposed site and interaction-dependent equations to estimate R_F and R_m modification factors for SSI systems (Eqs. (11) and (15)) can be obtained based on standard IBC-2012 [28] design spectra for different soil classes and, therefore, can be directly used in practical applications. Here, the following design procedure is suggested for performance-based seismic design of flexible-base structures:

Step 1: The MDOF structure is initially designed based on fixed-base behaviour (i.e. by ignoring the effects of SSI) for gravity and seismic loads according to a design code such as IBC-2012 [28].

Step 2: The properties of the representative SDOF structure of the fixed-base MDOF system are then calculated, including the fundamental period T_n and slenderness ratio s by using Eqs. (5) and (7), respectively. The structure-to-soil stiffness ratio a_0 and characteristic period T_0 are also obtained from Eq. (6) and Table 3, based on the expected shear wave velocity $V_{s,30}$ of the given site class.

Step 3: The base shear demand of the fixed-base elastic SDOF structure $V_{SDOF}(T_n, a_0 = 0, \mu = 1)$ is calculated from the elastic design spectrum by using the fundamental period T_n.

Step 4: To satisfy the predefined target ductility demand μ_t, the design base shear of the inelastic flexible-base MDOF structure $V_{MDOF}(T_n, a_0, s, \mu_{\max} = \mu_t)$ is directly calculated from Eq. (14), where R_F and R_M are obtained from Eqs. (12) and (15), respectively.

Step 5: The calculated base shear strength is distributed according to the design lateral load pattern used in Step 1, and the MDOF structure is designed based on the new seismic design loads. To achieve more reliable design solutions, the design process can be repeated from Step 2. However, the results of this study show that, if the initial structure is designed based on code-specified design load patterns, one iteration would be sufficient for practical applications.

The efficiency of the proposed performance-based design procedure is demonstrated by using several design examples. For this purpose, a number of typical 5, 10, 15 and 20-storey flexible-base buildings with, respectively, fixed-base fundamental periods of 0.61, 1.07, 1.48 and 1.87 sec and slenderness ratios of 1, 1.5, 2 and 3 were selected. The a_0 values were calculated based on the assumed shear wave velocities of 90, 270 and 560 m/s for site classes E, D and C, respectively. Following the proposed methodology, the buildings were designed for target ductility demands of 2, 4, 6 and 8, and were subsequently subjected to the set of 15 synthetic earthquakes representing the IBC-2012 [28] design spectrum corresponding to the selected site class (see Fig. 3). The actual ductility demands, averaged for the 15 spectrum-compatible earthquakes in each set, are compared with the target values in Fig. 16. The comparison shows a very good agreement between the actual and expected ductility demands, which proves the reliability of the proposed design procedure for performance-based design of flexible-base multi-storey buildings.

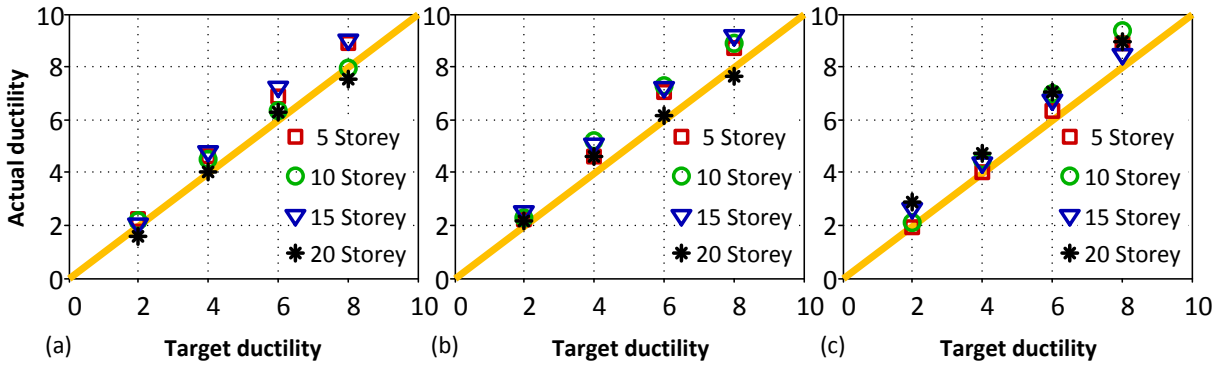

Fig. 16. Comparison of the actual ductility demands with target ductility ratios for (a) Site Class C, (b) Site Class D, (c) Site Class E.

8 Conclusions

The effects of soil-structure interaction on the strength and ductility demands of multi-storey shear buildings were investigated. A large number of 1, 5, 10, 15 and 20-storey structures with a wide range of fundamental period, target ductility demand, slenderness ratio and structure-to-soil stiffness ratio were subjected to three sets of synthetic spectrum-compatible earthquakes corresponding to different soil classes. Based on the results of this study, the following conclusions can be drawn:

- Using concentric, rectangular, trapezoidal, parabolic and code-specified design load patterns (IBC-2012 and Eurocode-8) to design flexible-base MDOF structures showed that the code-specified load patterns are, in general, more suitable for long period structures, whereas the trapezoidal pattern provides the best design solution for short period flexible-base structures.
- For common building structures with low-to-medium ductility demands under spectrum-compatible earthquakes, increasing structure-to-soil stiffness ratio a_0 can considerably reduce (up to 60%) the structural strength demand in comparison to similar fixed-base structures. This implies that for most typical buildings considering SSI in the design process can lead to more cost-effective design solutions with less structural weight.
- To satisfy a target ductility demand for SSI systems with similar fixed-base fundamental periods and structure-to-soil stiffness ratios, the total structural strength increases by increasing the slenderness ratio s, especially in the short period range (i.e. T_n<0.5sec).

- By using the results of more than 40,000 SDOF and MDOF systems under spectrum compatible earthquakes, simple equations were introduced to calculate the site and interaction-dependent MDOF modification factor (R_M) and strength reduction factor (R_F) for flexible-base structures by taking into account the effects of both SSI and inelastic hysteretic behaviour of the structure.
- Based on the results of this study, a practical performance-based design procedure was proposed to calculate the strength demand of an MDOF flexible-base structure to satisfy a predefined target ductility demand. The reliability and efficiency of the method was demonstrated by using several design examples.

REFERENCES

[1] ASCE/SEI 41-13. Seismic evaluation and retrofit of existing buildings. American Society of Civil Engineers, Reston, Virginia; 2013.
[2] CEN. Eurocode 8: Design of structures for earthquake resistance. Part 5: Foundations, retaining structures and geotechnical aspects. EN 1998-5:2004 Comité Européen de Normalisation, Brussels, Belgium: CEN; 2004.
[3] Veletsos AS, Meek JW. Dynamic behaviour of building-foundation systems. Earthquake Engineering and Structural Dynamics. 1974;3:121-38.
[4] Elnashai AS, McClure DC. Effect of modelling assumptions and input motion characteristics on seismic design parameters of RC bridge piers. Earthquake Engineering and Structural Dynamics. 1996;25:435-63.
[5] Ciampoli M, Pinto PE. Effects of soil-structure interaction on inelastic seismic response of bridge piers. Journal of Structural Engineering. 1995;121:806-14.
[6] Bielak J. Dynamic response of non-linear building-foundation systems. Earthquake Engineering and Structural Dynamics. 1978;6:17-30.
[7] Priestley MJN, Park R. Strength and ductility of concrete bridge columns under seismic loading. Aci Struct J. 1987;84.
[8] Mylonakis G, Gazetas G. Seismic soil-structure interaction: beneficial or detrimental? J Earthq Eng. 2000;4:277-301.
[9] Avilés J, Pérez-Rocha LE. Soil-structure interaction in yielding systems. Earthquake Eng Struct Dyn. 2003;32:1749-71.
[10] Avilés J, Pérez-Rocha LE. Influence of foundation flexibility on R_μ and C_μ factors. J Struct Eng. 2005;131:221-30.
[11] Ghannad MA, Jahankhah H. Site-dependent strength reduction factors for soil-structure systems. Soil Dyn Earthquake Eng. 2007;27:99-110.
[12] Jarernprasert S, Bazan-Zurita E, Bielak J. Seismic soil-structure interaction response of inelastic structures. Soil Dyn Earthq Eng. 2013;47:132-43.
[13] Santa-Ana PR, Miranda E. Strength reduction factors for multi-degree-of-freedom systems. Proceedings of the 12th world conference on Earthquake Engineering. Auckland, New Zealand, 2000.
[14] Ganjavi B, Hao H. Strength reduction factor for MDOF soil–structure systems. The Structural Design of Tall and Special Buildings. 2014;23:161-80.
[15] Raychowdhury P. Seismic response of low-rise steel moment-resisting frame (SMRF) buildings incorporating nonlinear soil–structure interaction (SSI). Eng Struct. 2011;33:958-67.
[16] Aydemir ME, Ekiz I. Soil–structure interaction effects on seismic behaviour of multistorey structures. Eur J Environ Civ En. 2013;17:635-53.
[17] Diaz O, Mendoza E, Esteva L. Seismic ductility demands predicted by alternate models of building frames. Earthq Spectra. 1994;10:465-87.
[18] Hajirasouliha I, Doostan A. A simplified model for seismic response prediction of concentrically braced frames. Adv Eng Softw. 2010;41:497-505.
[19] Ehlers G. The effect of soil flexibility on vibrating systems. Beton und Eisen. 1942;41:197-203.
[20] Meek JW, Wolf JP. Cone models for homogeneous soil. I. Journal of geotechnical engineering. 1992;118:667-85.

[21] Wolf JP. Foundation vibration analysis using simple physical models: Englewood Cliffs (NJ): Prentice Hall; 1994.
[22] Meek JW, Wolf JP. Material damping for lumped-parameter models of foundations. Earthquake Eng Struct Dyn. 1994;23:349-62.
[23] Veletsos AS, Nair V. Seismic interaction of structures on hysteretic foundations. J Struct Div. 1975;101:109-29.
[24] Luco JE, Lanzi A. Approximate soil-structure interaction analysis by a perturbation approach: The case of stiff soils. Soil Dyn Earthq Eng. 2013;51:97-110.
[25] Veletsos AS, Verbič B. Vibration of viscoelastic foundations. Earthquake Eng Struct Dyn. 1973;2:87-102.
[26] ATC-40. Seismic evaluation and retrofit of concrete buildings. Applied Technology Council, Redwood City, CA; 1996.
[27] FEMA-356. Prestandard and Commentary for the Seismic Rehabilitation of Buildings. Federal Emergency Management Agency, Washington, DC; 2000.
[28] IBC. International Building Code. International Code Council, INC, Country Club Hills, USA: IBC-2012; 2012.
[29] FEMA-450. NEHRP Recommended Provisions for Seismic Regulations for New Buildings and Other Structures. Federal Emergency Management Agency, Washington, DC; 2003.
[30] Hajirasouliha I, Pilakoutas K. General Seismic Load Distribution for Optimum Performance-Based Design of Shear-Buildings. J Earthq Eng. 2012;16:443-62.
[31] ASCE/SEI 7-10. Minimum design loads for buildings and other structures. American Society of Civil Engineers, Reston, Virginia; 2010.
[32] Gasparini DA, Vanmarcke E. SIMQKE: A Program for Artificial Motion Generation: User's Manual and Documentation: MIT Department of Civil Engineering; 1976.
[33] Stewart JP, Fenves GL, Seed RB. Seismic soil-structure interaction in buildings. I: Analytical methods. J Geotech Geoenviron. 1999;125:26-37.
[34] Stewart JP, Seed RB, Fenves GL. Empirical evaluation of inertial soil-structure interaction effects: Pacific Earthquake Engineering Research Center; 1998.
[35] MATLAB. The MathWorks. Inc, Natick, Massachusetts, United States. 2014.
[36] Newmark NM. A method of computation for structural dynamics. Journal of the Engineering Mechanics Division. 1959;85:67-94.
[37] Moghaddam H, Mohammadi RK. Ductility reduction factor of MDOF shear-building structures. J Earthq Eng. 2001;5:425-40.
[38] Ganjavi B, Hao H. Effect of structural characteristics distribution on strength demand and ductility reduction factor of MDOF systems considering soil-structure interaction. Earthq Eng Eng Vib. 2012;11:205-20.
[39] Miranda E, Bertero VV. Evaluation of strength reduction factors for earthquake-resistant design. Earthquake Spect. 1994;10:357-79.
[40] Moghaddam H, Hajirasouliha I. Toward more rational criteria for determination of design earthquake forces. Int J Solids Struct. 2006;43:2631-45.
[41] Veletsos AS, Verbic B. Dynamics of elastic and yielding structure-foundation systems. Proceedings of the 5th world conference on Earthquake Engineering. Rome, Italy, 1974. p. 2610-3.
[42] Maravas A, Mylonakis G, Karabalis DL. Simplified discrete systems for dynamic analysis of structures on footings and piles. Soil Dyn Earthquake Eng. 2014;61:29-39.
[43] Vidic T, Fajfar P, Fischinger M. Consistent inelastic design spectra: strength and displacement. Earthquake Eng Struc. 1994;23:507-21.
[44] Nassar AA, Krawinkler H. Seismic demands for SDOF and MDOF systems: John A. Blume Earthquake Engineering Center, Department of Civil Engineering, Stanford University; 1991.
[45] Miranda E. Strength reduction factors in performance-based design. Proceedings of EERC-CUREe Symposium, Berkeley, CA, 1997.